Optimization of dielectric substrate for a 7 T radiative antenna: role of surface waves

Ozlem Ipek[1], J. J.W. Lagendijk[1], and C.A.T. van den Berg[1]
[1]*Radiotherapy, UMC Utrecht, Utrecht, Utrecht, Netherlands*

Introduction: In a transmit array for ultra-high field prostate imaging, the aim is to generate a high transmit signal at the prostate [1-2]. Since the prostate depth is approximately one wavelength at 300 MHz, it is located outside the resonant near-field that MR coils were traditionally designed on. Thus, for sufficient RF signal penetration at depth, a radiative design is more favorable than classical near field coupling. An example of a radiative antenna is the single-side adapted dipole antenna [3]. It consists of a dipole antenna placed on a high-dielectric substrate. To further improve the field efficiency at the target region, further optimization of the antenna is required. In particular, the dimensions and properties of the substrate will be important in achieving optimal efficiency. In the literature, the effect of substrate thickness and relative permittivity has been extensively studied for printed circuit board dipole antennas [4]. As the permittivity of the substrate increases, power can be coupled into TM or TM modes propagating in the substrate which forms a dielectric slab waveguide. This phenomenon occurs when the permittivity and height of the substrate are large enough to make these modes above cut off. These so-called surface waves create a loss mechanism in printed circuit board antennas. In this study we investigate their role for the B_1^+ signal penetration of a radiative antenna at 7T.

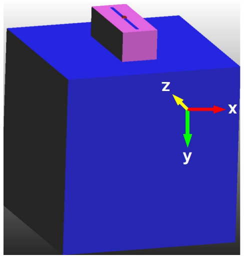

Figure 1: Radiative antenna (pink) placed on a phantom.

Method: Surface waves appear, if 1) they are excited, i.e. their field orientations match with the field orientations of the RF probe and 2) the optical thickness ($\sqrt{\varepsilon_r} \cdot d$) of the substrate is greater that the various cut off thicknesses of all modes. The electric dipole placed on the dielectric substrate can, given its electric and magnetic field orientations, only excite odd and even TM modes in the substrate. Cut off frequencies of various TM modes are given in Table 1. Note that the lowest order odd TM does not have a cut off frequency. FDTD package SEMCAD X (SPEAG, Schmid & Partner Engineering, Zurich, Switzerland) was used for numerical simulations. Various substrate permittivities (ε_r=20, 36, 90, 110, σ:0.001 S/m), and substrate dimensions were simulated. The height of the substrate was varied from 1 to 19 cm with 1 cm steps. The substrate width and length in these simulations were 5 cm and 15.3 cm, respectively. In an additional simulation run, the width of the substrate was changed from 1 to 30 cm with 1 cm steps, where the height and length were kept at 5 cm and 15.3 cm, respectively. The radiative elements were placed on a phantom (ε_r=34, σ:0.47 S/m, 30 ×30 ×30 cm^3) (Figure 1). All radiative elements were tuned at 300 MHz and matched by using a capacitor and an inductor. To visualize the surface waves clearly, in addition to a finite substrate, also a very large substrate (5 cm high, 2.5 m wide and long) was simulated.

	ε_r=36	ε_r=90	ε_r=110
1st odd TM	No cut-off		
1st even TM	84	53	48
2nd odd TM	-	106	96
3rd even TM	-	159	144
3rd odd TM	-	-	192

Table1: The waveguide modes in the substrate with dielectric permittivities 36, 90 and 110 at different substrate thicknesses in mm.

Results and discussion: The existence of the surface waves is clearly shown for the large substrate with a dielectric constant of 90 (Figure 2 *b*). No surface waves are visible in the substrate with a dielectric constant of 36 (*Figure 2a*).

The Poynting vector along the interface (Sx, related to lateral energy transport Figure 3 *a-b*) at 2 cm depth, the Poynting vector directed into phantom (Sy) at 10 cm depth (Figure 3 *c-d*), and the B_1^+ field at 10 cm depth (Figure 3 *e-f*) are depicted. The Poynting vector at 10 cm depth of the phantom for the substrate with ε_r=20 shows sinusoidal behavior as a function of the substrate thickness (Figure 3 *c*). This arises from interference undulations between the directly transmitted waves and waves that make a roundtrip in the substrate due to reflections, before being transmitted in the substrate [5]. Around a substrate thickness of 80 mm for ε_r=36, deviations in the sinusoidal behavior are visible. In Figure 3 *a*, a discontinuity is visible at the cut off height of the 1st even TM mode. For higher permittivities, discontinuities in Sx vs. height graphs coincide with cut off heights of 1st even TM surface mode (Figure 2 *b*). Noted that the appearance of this surface mode results also in discontinuities in the Sy vs. height and B_1^+ vs. height plots (Figure 3 *d*, *f*). The laterally propagating surface modes do not necessarily represent a loss mechanism for the power flow into phantom. The surface modes partly reflect at the lateral substrates edges, setting up a lateral, standing wave pattern in the substrate. This is illustrated by Figure 4 which shows a dampened sinusoidal behavior of B_1^+ field at depth with substrate width. This arises due to constructive interferences between reflected surface waves at each lateral side. The curve dampens for larger width since a surface wave during propagation looses part of its energy due to leakage into the phantom. This leakage is maximized when the surface wave interfere constructively creating higher B_1^+ field at depth.

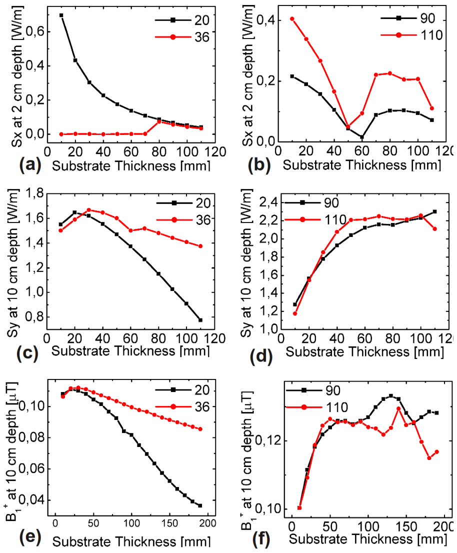

Figure 3: The x component of the Poynting vector at 2 cm (a,b) and y component of the Poynting vector at 10 cm (c,d) depth, and B_1^+ at 10 cm depth (e,f) for substrates with a permittivity of 20, 36 (a,c,e) and 90,110 (b,d,f) are shown as a function of the substrate thicknesses.

Conclusion: Laterally propagating surface waves are important for radiative antennas employing a dielectric substrate. Optimal incoupling of RF signal is strongly determined by this phenomenon.

References:(1) Metzger G J *et al* 2010 *Magn. Reson. Med.* **64** 1625. (2) van den Bergen B *et al* 2011 *NMR Biomed.* **24** 358 (3) Raaijmakers A J E *et al* 2011 *Magn. Reson. Med.* **66** 1488 (4) Katehi, P.B. 1983 *IEEE Trans.on Antennas and Propagation* **AP-31**, No 1. (5) Novothny L & Hecht B Principles of nano-optics, Cambridge 2006

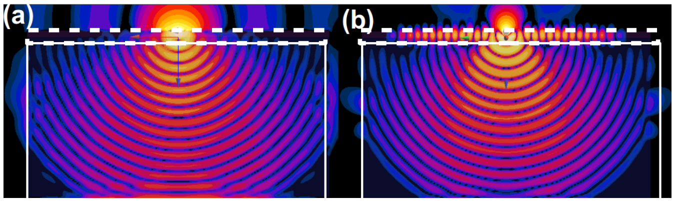

Figure 2: Transverse slice of the real Modulus E field for the infinite substrate with dielectric constant of 36(a) and 90 (b) on an infinitely big phantom.

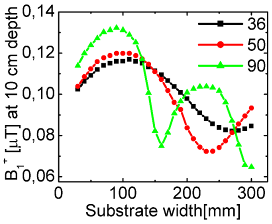

Figure 4: The change in B_1^+ at 10 cm depth as a function of increase in substrate width with ε_r of 36, 50 and 90